Considerations in the Use of Coplanar Waveguide For Millimeter-Wave Integrated Circuits

ROBERT W. JACKSON, MEMBER, IEEE

Abstract — **Using a full-wave analysis, coplanar waveguide (CPW) transmission line is compared to microstrip in terms of conductor loss, dispersion, and radiation into parasitic modes. It is shown that, on a standard 0.1-mm semiconductor at 60 GHz, the dimensions of CPW can be chosen to give better results in terms of conductor loss and dispersion than microstrip. A calculation of parasitic mode generation is presented for CPW on a semiconductor for an open substrate, for a substrate suspended above a ground plane, and for substrates separated from a ground plane by quartz.**

I. Introduction

FOR MANY YEARS, monolithic microwave integrated circuits have predominantly used microstrip transmission lines. At microwave frequencies, microstrip is well understood and flexible in that a large number of circuit elements can be made with it. However, for integrated circuits operating at millimeter-wave frequencies, it may not be the medium of choice. One disadvantage is that via holes are required to ground active devices. At millimeter-wave frequencies, these vias can introduce significant inductance and degrade circuit performance.

Coplanar waveguide (CPW) has been suggested as an alternate to microstrip [1], but it has not been widely used due to the mistaken assumption that it has inherently higher conduction loss than microstrip. Its principal advantage is that it is well suited for use with field-effect transistors, especially at millimeter-wave frequencies where RF grounding must be close to the device. Via holes are not necessary and fragile semiconductors need not be made excessively thin [8], [12]. Ground connections can conveniently be made at the substrate edge.

Determining conductor loss in an absolute sense is difficult for planar lines such as microstrip or CPW. It depends to a large extent on conductor surface roughness, which can vary from substrate to substrate. It also depends upon the behavior of current crowded near the edge of etched conductor. Instead of including a roughness factor and determining loss absolutely, this paper compares CPW and microstrip in terms of conductor loss by using a full-wave analysis and a method proposed by Lewin [2] for calculating losses including edge effects. These calculations show the size which a CPW must be in order to compete with microstrip in terms of loss over a large impedance range on semiconductor substrate. Most calculations of planar circuit structures have used quasi-static methods [3], [4]; however, at millimeter-wave frequencies, a full-wave analysis [5], [6] is necessary because dimensions are often a significant fraction of a dielectric wavelength. The details of the analysis are briefly described in Section II. The resulting dimensions can then be used to compare CPW dispersion to that of microstrip. The loss and dispersion comparison is discussed in Section III.

At millimeter-wave frequencies, radiation loss to parasitic modes such as surface waves can occur. This loss depends upon substrate thickness, substrate permittivity, and the cross section (size) of the transmission line being considered. The sizes of CPW determined in Section III can now be used to calculate the parasitic radiation loss characteristics of CPW in different mounting configurations.

Often, CPW is considered to have free space above and below the substrate, but in practical applications a ground plate is placed some distance from the substrate on at least one side. This plate isolates the coplanar waveguide from the lower half space. It is, however, awkward to suspend a fragile semiconductor substrate and therefore mounting the substrate directly on a ground plate (grounded coplanar waveguide) is often suggested. In this structure, for fairly large chips at millimeter-wave frequencies, a parallel plate mode can exist which has a phase velocity that is less than that of the desired grounded coplanar waveguide mode. Leaky waves then result as well as mode conversion at discontinuities. A better possibility is to mount the semiconductor substrate on a low-permittivity material such as quartz and then mount the entire assembly on a ground plate. The low-permittivity material then supports the semiconductor and raises the parallel plate phase velocity to a point where much less mode conversion occurs. In Section IV, a full-wave analysis of a short-circuited coplanar line shows the degree to which a parallel plate mode is excited for various plate spacings.

II. Infinite Line Analysis

Full-wave analysis techniques are well known for infinitely long transmission lines [5], [6]. The techniques presented in this section outline the methods used for

Manuscript received April 2, 1986; revised July 1, 1986. This work was supported in part by the General Electric Company and by the Air Force Office of Scientific Research.

The author is with the Department of Electrical and Computer Engineering, University of Massachusetts, Amherst, MA 01003.

IEEE Log Number 8610549.

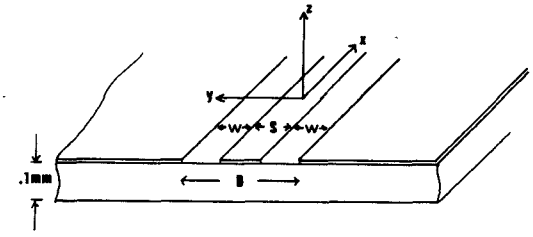

Fig. 1. Structure of the coplanar waveguide transmission line.

calculation of the loss, impedance, and dispersion in CPW. The same techniques were used to obtain the same quantities in microstrip.

For coplanar waveguide, currents on the $z = 0$ plane (see Fig. 1) are determined by the slot fields according to the relation

$$\begin{bmatrix} J_y(y) \\ J_x(y) \end{bmatrix} = \frac{1}{2\pi}\int_{-\infty}^{\infty} dk_y \begin{bmatrix} \tilde{g}_{yy} & \tilde{g}_{yx} \\ \tilde{g}_{xy} & \tilde{g}_{xx} \end{bmatrix} \begin{bmatrix} \tilde{E}_y(k_y) \\ \tilde{E}_x(k_y) \end{bmatrix} \exp(jk_y y) \tag{1}$$

where an $\exp(-j\beta x)$ dependence has been suppressed. The $\tilde{g}_{ij}$ (see Appendix) are the Fourier transform of the Green's function and are dependent upon β and k_y. Following the work by Jansen [5] and Itoh [6], we expand $E_y(y)$ and $E_x(y)$ in terms of the functions

$$E_y(y) = \sum_{n=0}^{N} A_n \frac{\cos(n\pi[u/w + 1/2])}{\sqrt{1-(2u/w)^2}}$$

$$E_x(y) = \sum_{n=1}^{N} B_n \frac{\sin(n\pi[u/w + 1/2])}{\sqrt{1-(2u/w)^2}}$$

$$u = |y| - (s+w)/2, \quad -w/2 < u < w/2. \tag{2}$$

These functions show the proper behavior at the edges and are necessary for loss and impedance calculations. Weighted moments of the currents in (1) are forced to zero with weighting functions which are the same as the testing functions. As usual, β is varied until nontrivial values of A_n and B_n can exist. The A_n and B_n can then be used with (1) and (2) to determine J_x and J_y everywhere on the conductors.

Characteristic impedance is defined using a voltage–current definition

$$Z_c = V \cdot \left[2\int_0^s dy J_x(y)\right]^{-1} \tag{3}$$

where V is the line integral of the E_y field across the gap. One could also use a power–voltage definition, but it turns out that the difference is insignificant for the parameter range of interest in this discussion. At low frequencies, the impedances calculated compare favorably with those calculated using a quasi-static approximation. Although a completely open substrate is assumed in this section, impedances of CPW with a ground plate have also been calculated, and as long as the plate is not touching the substrate it is not difficult to choose the physical parameters of the CPW such that the impedance is very insensitive to plate spacing. This lack of sensitivity is not surprising since the capacitance between the center conductor and the ground plate is small due to the presence of an air space. A voltage–current definition is also used for microstrip where the current is the x-directed current on the strip and the voltage is the line integral of the E_z field under the strip averaged over the strip width.

CPW conductor loss is determined from the formula

$$\alpha = C\frac{Z_c}{V^2}\left[\int_0^{s/2-\Delta} dy + \int_{s/2+w+\Delta}^{\infty} dy\right] \cdot \left[|J_y^u|^2 + |J_x^u|^2 + |J_y^l|^2 + |J_x^l|^2\right] \tag{4}$$

where $\Delta = t/290$, t is the conductor thickness, and C is a constant that includes surface resistivity. The choice of Δ is made according to Lewin's work [2] in order to avoid the nonintegrable singularity at the edge of the zero-thickness conductor assumed in the full-wave analysis. The u and l superscripts refer to the current on the upper and lower sides of the conductor. These currents were calculated using (1) except that the Green's function is replaced by one that determines the current only on the upper (or lower) sides of the conductor (see Appendix). The integrals in (4) are evaluated numerically and the currents at each y value of the integrand are evaluated from numerical integration of (1). This last integration is very slow to converge for points near the conductor edges, and one must subtract the asymptotic value of the integrand and integrate it analytically.

Dielectric loss is calculated using the standard formula [7] and is only a small part of the total loss (about 10 percent).

III. Comparison Results

For a given substrate thickness and permittivity, microstrip impedance is varied by changing only the strip width. In contrast to this, CPW impedance depends roughly upon the ratio of inner conductor width to total cross section. Thus, CPW of several different sizes could have the same impedance. However, the smaller cross sections have higher conductor loss and thus a tradeoff exists between size and conductor loss.

Fig. 2 shows total loss (conductor and dielectric) plotted against impedance for microstrip and CPW on a 0.1-mm-thick substrate with a relative permittivity of 12.8 at 60 GHz. A conductor thickness of 3 μm is chosen. Copper conductor was assumed, but any other conductor would result in the same conclusions as far as comparisons are concerned. The coplanar waveguide impedance is varied by keeping a constant cross section (D) and changing the center conductor width. For microstrip, the only free parameter is the strip width. Strip widths were constrained to be between 10 and approximately 300 μm.

The figure shows that coplanar waveguide can have significantly less loss than microstrip over a broad range of impedances but especially at higher impedances. The impedance for minimum coplanar waveguide loss appears to be about 60 Ω for any of the chosen cross sections. The

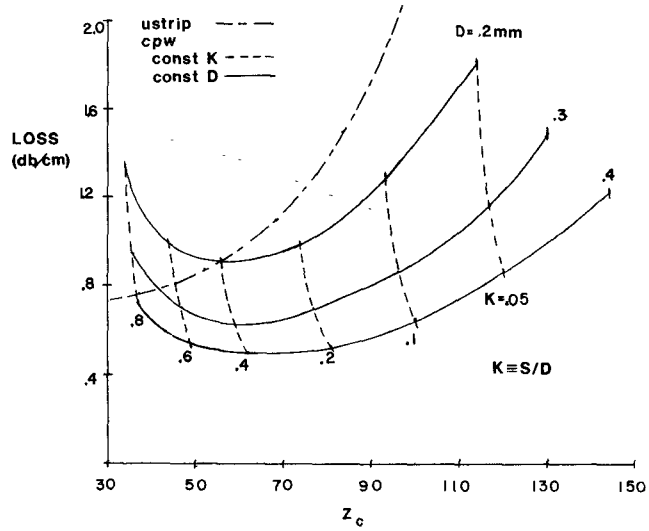

Fig. 2. Comparison of microstrip and coplanar waveguide losses for $\epsilon_r = 12.8$, $f = 60$ GHz, 0.1-mm substrate thickness, substrate loss tangent of 0.0006, and a 3-μm conductor thickness.

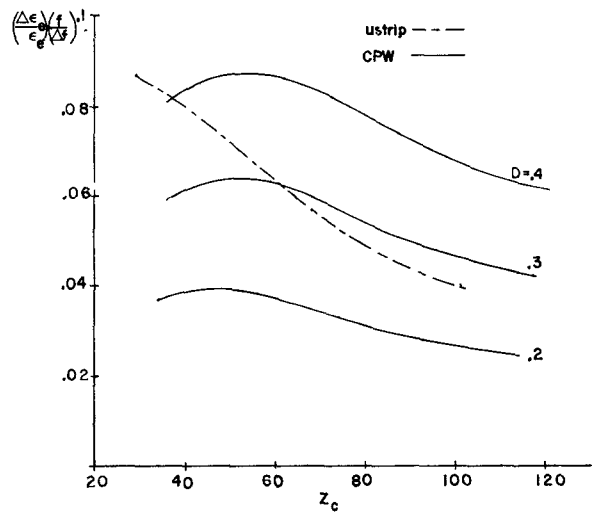

Fig. 3. Comparison of microstrip and coplanar waveguide dispersion.

microstrip width at minimum loss is about 300 μm, whereas the smallest coplanar waveguide cross section which will give the same loss is about 250 μm. Hence, sizes at the minimum loss impedance are similar. This could be an important consideration when long runs of line are contemplated.

The loss calculation shows the size that coplanar waveguide must be in order to compete with microstrip. For these sizes, Fig. 3 shows a comparison of dispersion for microstrip and coplanar waveguide. The fractional change in effective dielectric constant per fractional change in frequency is plotted against impedance. For frequencies near 60 GHz, the figure shows that coplanar waveguides with cross sections between 200 and 300 μm have as much or less dispersion than microstrip.

IV. Analysis of Parasitic Radiation Loss

At millimeter-wave frequencies on high-permittivity substrates, the radiation of unwanted (parasitic) modes can be a problem. For open structures, these parasitic modes are

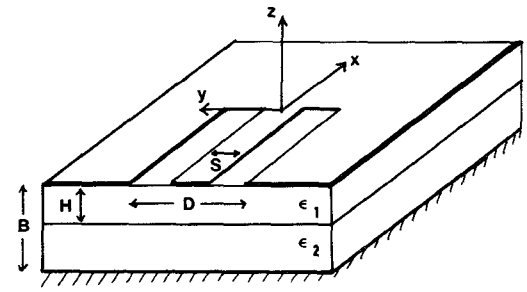

Fig. 4. Structure of the coplanar waveguide short circuit above two dielectric layers and ground plate. All layers are infinite in extent.

space waves and surface waves. In partially covered structures (a ground plate below the CPW, no sidewalls) the most likely mode to be excited is a parallel plate transmission line mode. Coplanar waveguide (odd mode) also has another parasitic mode (even mode) which can occur. The way to minimize conversion to this mode is to create symmetric circuits and thus not excite it or to use air bridges to short it out [8], [12].

In this section, the excitation of space, surface, and the parallel plate wave by a coplanar waveguide short is investigated. The structures which are considered (see Fig. 4) are the open substrate (no upper or lower plate, $\epsilon_2 = 1$), the partially covered substrate (a lower plate, no upper plate, $\epsilon_2 = 1$), and CPW mounted on quartz (a lower plate, no upper plate, $\epsilon_2 = 4.0$).

The analysis of losses from a microstrip open end and coplanar waveguide short circuit has been reported previously [9], [10]. In that work, the authors used a moment method technique to calculate the slot fields at the end of a coplanar waveguide. These fields were assumed to be transverse. The analysis which is presented here includes both longitudinal and transverse fields. In the previous analysis of the coplanar waveguide short, the slot fields were assumed to be symmetric around the slot centers. For tightly coupled slots, this can be inaccurate, as Jansen [5] points out. The possible asymmetry is allowed in the analysis which is now outlined.

Referring to Fig. 4, the currents on the $z = 0$ plane are related to slot fields by

$$\begin{bmatrix} J_y(x,y) \\ J_x(x,y) \end{bmatrix} = \frac{1}{(2\pi)^2} \iint_{-\infty}^{\infty} dk_x\, dk_y \begin{bmatrix} \tilde{G}_{yy} & \tilde{G}_{yx} \\ \tilde{G}_{xy} & \tilde{G}_{xx} \end{bmatrix} \cdot \begin{bmatrix} \tilde{E}_y(k_x,k_y) \\ \tilde{E}_x(k_x,k_y) \end{bmatrix} \cdot \exp\left(jk_x x + jk_y y\right) \quad (5)$$

where, as in (1), the $\tilde{G}_{ij}$ are the two-dimensional Fourier transforms of the Green's function. The Green's functions for the open substrate and the partially covered substrate can be found in the Appendix. For the open substrate, these functions have poles corresponding to surface waves. For the partially closed substrate, poles also exist which correspond to parallel plate waveguide modes. For all the plate spacings discussed here, only the lowest order TM_0 mode can propagate. Space-wave radiation is included above and below the substrate for open CPW and only above in the partially open case.

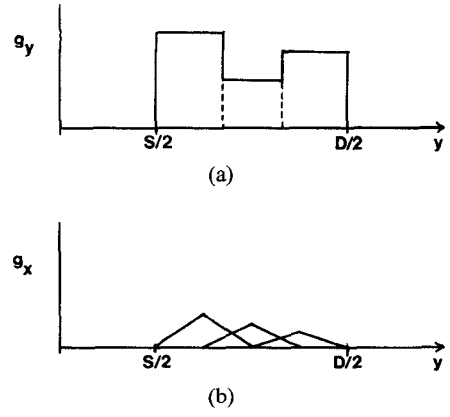

Fig. 5. Transverse variation of slot fields, for $y > 0$, (a) E_y, and (b) E_x.

The slot fields are expanded in terms of known functions multiplied by unknown constants

$$E_\alpha(x, y) = [(1+\Gamma)f_c(x) + j(1-\Gamma)f_s(x)]\, g_\alpha(y) + \sum_{n=1}^{N} A_{\alpha n} f(x - x_n) g_\alpha(y) \quad (6)$$

where

$$f_s(x) = \begin{cases} \sin \beta x, & 0 > x > -m\pi/\beta \\ 0, & \text{otherwise} \end{cases}$$

$$f_c(x) = f_s(x + \pi/(2\beta))$$

$$f(x) = \begin{cases} \dfrac{\sin\left(\beta\left[L_p - |x|\right]\right)}{\sin \beta L_p}, & |x| < L_p \\ 0, & \text{otherwise} \end{cases}. \quad (7)$$

β is the propagation constant on the infinite line, the length of the piecewise sinusoid is $L_p = \pi/(2N\beta)$, and m is the number of half wavelengths (5 or 6) which make up the finite length sinusoid $f_s(x)$. The x-dependence of the incident wave is $f_c - jf_s$ and the x-dependence of the reflected wave is $f_c + jf_s$. Piecewise sinusoids, $f(x - x_n)$, are all located near the end of the CPW. The reflection coefficient Γ and the constants A_{xn} and A_{yn} are unknown and are determined via the moment method solution. A total of $2N+1$ piecewise sinusoidal functions are used to test that the current calculated in (5) is zero in the slots.

The transverse dependence of the y-directed field $g_y(y)$ was made up of three pulse functions (Fig. 5(a)) and the transverse dependence of the x-directed field is made up of three triangle functions (Fig. 5(b)). The amplitudes of these functions as well as the propagation constant β are determined prior to the discontinuity calculation by the same full-wave analysis described in Section I except that the expansion functions in (2) are replaced by pulse and triangle functions. Due to the similarity of the expansion functions to one another in the Fourier transform domain, the computation is efficient and the amplitudes and propagation constants can be quickly calculated. The propagation constants so calculated are within 1 percent of those calculated using the expansion modes in (2). Once the amplitudes are computed, $g_\alpha(y)$ is fixed for the remainder of the discontinuity calculation. By using this type of function for $g_\alpha(y)$, the asymmetry in the slot fields can be included in the analysis of the short-circuit discontinuity.

Sufficient piecewise sinusoidal modes were used such that the end resistance and length extension converge to within an estimated 5 percent of their final value. Although length extension was not a goal of this calculation, this method produced results which were within 10 percent of those calculated by Jansen [11].

Loss from an open-ended microstrip was calculated in a similar manner except that the transverse variation of the x- and y-directed strip currents were, respectively,

$$\frac{1}{\sqrt{1-(2y/w)^2}} \quad \text{and} \quad \frac{\sin(\pi[y/w + 1/2])}{\sqrt{1-(2y/w)^2}} \quad (8)$$

where w is the microstrip width.

V. Results of Discontinuity Loss Calculations

In this section, parasitic radiation loss results are presented for a short-circuit CPW on a semiconductor substrate in an open structure, separated from a ground plate by free space, and separated from a ground plate by quartz.

Fig. 6 compares power lost due to space-wave and surface-wave radiation from a microstrip open end and a coplanar waveguide short circuit on an open substrate. These values are obtained from end impedance calculations by the relationship

$$\frac{P_{\text{rad}}}{4P_{\text{incidence}}} \simeq \begin{cases} GZ_c, & \text{open end microstrip} \\ RY_c, & \text{short-circuit CPW} \end{cases}$$

where $G(R)$ is the real part of the end admittance (impedance). Coplanar waveguide size (D) is chosen in accordance with the conductor loss results in the second section. A $\epsilon_r = 12.8$ substrate of thickness $H = 0.02\lambda_0$ is assumed. Impedances are varied by varying the center strip width of the CPW while holding the total cross section constant. The coplanar waveguide short evidently radiates much less energy than the microstrip open.

It should be noted that it is quite possible that a CPW open circuit will radiate more energy than a CPW short circuit, and so it may be unfair to say that coplanar waveguide always radiates less than microstrip. However, the CPW short is, arguably, more representative of many CPW discontinuities (steps and turns, for example) than the open. In addition, since the CPW short is approximately made up of two abruptly terminated oppositely directed magnetic currents, it is a rough dual to the microstrip open which consists of two abruptly terminated oppositely directed electric currents (the strip current and its image). Thus, it seems that comparing microstrip and coplanar waveguide in this manner is reasonable.

Fig. 7(a) and (b) plots loss from a short-circuited CPW line versus plate separation for a partially covered CPW. A constant cross section ($D = 3H$) and strip width ($S = 1.2H$) corresponding to roughly a 60-Ω impedance is assumed.

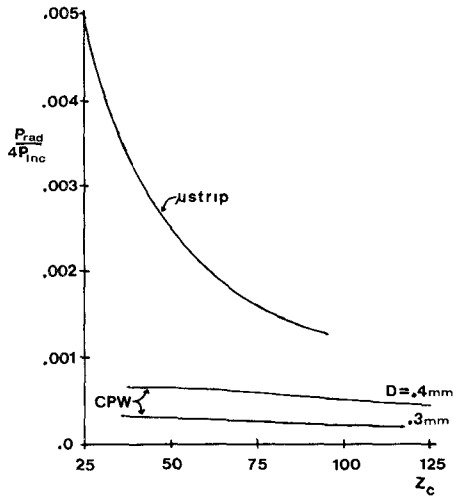

Fig. 6. Comparison of microstrip and coplanar waveguide discontinuity loss for $\epsilon_r = 12.8$, $f = 60$ GHz, and 0.1-mm substrate thickness.

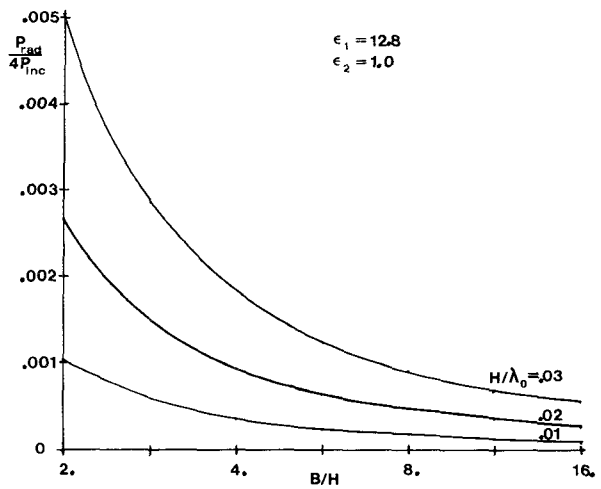

(a)

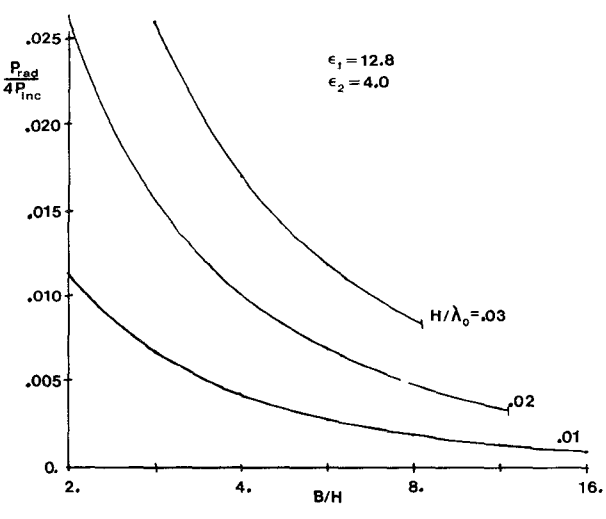

(b)

Fig. 7. Power loss at a coplanar waveguide short circuit with $S = 1.2H$, $D = 3H$. (a) Free space between the substrate and ground plate (b) Quartz between the substrate and ground plate.

The cross section chosen corresponds to the size determined from the conductor loss calculation at 60 GHz. Three different frequencies are plotted (corresponding to 30, 60, and 90 GHz if a 0.1-mm substrate is used).

The plate spacings are small enough that only the lowest parallel plate waveguide mode propagates and therefore is the only source of radiated loss below the CPW. If the plate spacing were increased, eventually more parallel plate modes could be excited and more poles would appear in the Green's function. Above the CPW, space-wave radiation is the only source of radiative loss.

If a 50-Ω microstrip open end is taken as a gauge, then Fig. 6 shows that on a 0.1-mm GaAs substrate about 1 percent of the energy incident upon it will be radiated as surface and space waves at 60 GHz. To ensure that less energy is radiated from a short-circuit CPW at the same frequency, Fig. 7(a) shows that the plate spacing must be greater than about two substrate thicknesses.

Fig. 7(b) shows how the loss changes if a dielectric such as quartz is used between the substrate and the ground plate. The loss increases dramatically and the plate spacing which formerly gave 1-percent loss now gives about 8 percent. This loss can be decreased significantly by increasing the spacing (quartz thickness). But above a certain point the first TE parallel plate waveguide mode starts propagating. The results presented in Figs. 6 and 7 are for plate spacings which preclude propagation of this added mode.

When the plate spacing decreases (causing the plate to approach the bottom of the substrate), the phase velocity of the parallel plate mode eventually becomes slower than that of the CPW mode on an infinite line. Leakage can then result from the line prior to the short-circuit discontinuity. The results in Fig. 7(a) and (b) do not include any spacings which are small enough for leaky modes.

VI. Conclusions

It has been shown that, at millimeter-wave frequencies, coplanar waveguide can be equal to or better than microstrip when loss and dispersion on GaAs substrate are used as a basis for comparison. Minimum loss for a given coplanar waveguide cross section occurs at about a 60-Ω impedance, whereas the minimum loss for microstrip occurs at about 25 Ω. The physical sizes at these minimum loss impedances are similar. For higher impedances, coplanar waveguide can give much smaller loss but will take up more space than the same impedance microstrip line.

Using the coplanar waveguide sizes required to make conductor loss comparable to that of microstrip, we have calculated discontinuity radiation loss from a short-circuit coplanar waveguide on a semiconductor substrate in an open structure, a structure suspended over a ground plate, and one mounted on quartz. Radiated loss (including surface waves) is very small for an open substrate. For a substrate separated from a ground plate by free space, radiation into a parallel plate transmission line mode can be kept to very small levels by separating the plate from

the substrate by a couple of substrate thicknesses. For a *substrate separated* from a ground plate by a dielectric material such as quartz, radiation into the parallel plate mode is increased substantially and a significantly larger plate separation is necessary. Reactive circuit characteristics such as impedance and length extension were very insensitive to plate spacings beyond two or three substrate thicknesses and were also insensitive to small variations in quartz permittivity. Therefore, circuits in a semiconductor substrate which are mounted on low-permittivity material will not be sensitive to that material except for parasitic radiation effects.

The results presented assume a substrate with no sides. This should be a valid assumption for large chips at millimeter-wave frequencies. Radiated parallel plate energy could then be expected to couple to other circuits on the chip or radiate at the edges. Infinitely long coplanar waveguide structures which have ground plates too close to or on the substrate (grounded coplanar waveguide) can leak energy and should be avoided.

Coplanar waveguide compared to microstrip have the following disadvantages: size, the possibility that an even mode can be excited at nonsymmetric discontinuities, and possibly poorer heat transfer for active devices. Also, the variety of circuit elements available for microstrip is not yet available in coplanar waveguide.

The advantages of coplanar waveguide include: easier construction using thicker substrates and no via holes, good grounding for integrated active devices, less radiation at discontinuities, and, in some cases, lower conductor loss.

Appendix

For an open substrate, the following functions are the Fourier transform of the Green's function which relates an infinitesimal slot electric field (magnetic current) at $x = y = z = 0$ to the electric current on the lower side of a conductor on the $z = 0$ plane (see Fig. 1):

$$\tilde{G}'_{yy}(k_x, k_y, \epsilon_r) = \frac{k_x^2 A + (\epsilon_r k_0^2 - k_x^2) B}{-\omega\mu}$$

$$\tilde{G}'_{xy}(k_x, k_y, \epsilon_r) = \frac{k_x k_y (A - B)}{\omega\mu} \tag{A1}$$

where

$$A = \frac{k_1(1-\epsilon_r)}{\mathrm{TM\,TE}}$$

$$B = \frac{k_1 \cos[k_1 H] + \epsilon_r k_2 j \sin[k_1 H]}{k_1 \mathrm{TM}}$$

where

$$\mathrm{TE} = k_1 \cos[k_1 H] + jk_2 \sin[k_1 H],$$

$$\mathrm{TM} = \epsilon_r k_2 \cos[k_1 H] + jk_1 \sin[k_1 H]$$

$$k_2^2 = k_0^2 - \beta^2, \quad k_1^2 = \epsilon_r k_0^2 - \beta^2, \quad \beta^2 = k_x^2 + k_y^2$$

and H is the substrate thickness. Except for loss calculations, only the sum of the currents on the lower and upper sides is of interest

$$\begin{aligned}
\tilde{G}_{yy}(k_x, k_y) &= \tilde{G}'_{yy}(k_x, k_y, \epsilon_r) + \tilde{G}'_{yy}(k_x, k_y, 1) \\
\tilde{G}_{xy}(k_x, k_y) &= \tilde{G}'_{xy}(k_x, k_y, \epsilon_r) + \tilde{G}'_{xy}(k_x, k_y, 1) \\
\tilde{G}_{yx}(k_x, k_y) &= \tilde{G}_{xy}(k_x, k_y) \\
\tilde{G}_{xx}(k_x, k_y) &= \tilde{G}_{yy}(k_x \to k_y, k_y \to k_x).
\end{aligned} \tag{A2}$$

For an infinite line, the x variation is $\exp[-j\beta x]$ and therefore the Green's functions used in (1) are

$$\begin{aligned}
&\tilde{g}_{yy}(\beta, k_y) = \tilde{G}_{yy}(-\beta, k_y), \quad \tilde{g}_{yx}(\beta, k_y) = \tilde{G}_{xy}(-\beta, k_y) \\
&\tilde{g}_{xy}(\beta, k_y) = \tilde{G}_{xy}(-\beta, k_y), \quad \tilde{g}_{xx}(\beta, k_y) = \tilde{G}_{yy}(k_y, -\beta).
\end{aligned} \tag{A3}$$

The structure in Fig. 2 includes a ground plate at $z = -B$ and is open for $z > 0$. In this case, the Fourier transform of the Green's function which relates the total current at a point on the $z = 0$ plane to a slot electric field at $x = y = z = 0$ is

$$\begin{aligned}
\tilde{G}_{pyy}(k_x, k_y) &= \tilde{G}'_{pyy}(k_x; k_y, \epsilon_1, \epsilon_2) + \tilde{G}'_{yy}(k_x, k_y, 1) \\
\tilde{G}_{pxy}(k_x, k_y) &= \tilde{G}'_{pxy}(k_x, k_y, \epsilon_1, \epsilon_2) + \tilde{G}'_{xy}(k_x, k_y, 1) \\
\tilde{G}_{pyx}(k_x, k_y) &= \tilde{G}_{pxy}(k_x, k_y) \\
\tilde{G}_{pxx}(k_x, k_y) &= \tilde{G}_{pyy}(k_x \to k_y, k_y \to k_x)
\end{aligned} \tag{A4}$$

where $\tilde{G}'_{ij}$ has been defined previously and

$$\tilde{G}'_{pyy}(k_x, k_y, \epsilon_1, \epsilon_2) = \frac{k_x^2 A_p + (\epsilon_1 k_0^2 - k_x^2) B_p}{-\omega\mu}$$

$$\tilde{G}'_{pxy}(k_x, k_y, \epsilon_1, \epsilon_2) = \frac{k_x k_y (A_p - B_p)}{\omega\mu}$$

where

$$A_p = j \frac{k_1 \sin[k_2(B-H)] \cos[k_2(B-H)](\epsilon_2 - \epsilon_1)}{\mathrm{TE}_p \mathrm{TM}_p}$$

$$B_p = \frac{\epsilon_2 k_1 \cos[k_2(B-H)] \cos[k_1 H] - \epsilon_1 k_2 \sin[k_2(B-H)] \sin[k_1 H]}{k_1 \mathrm{TM}_p}$$

$$\mathrm{TE}_p = jk_1 \sin[k_2(B-H)] \cos[k_1 H] + jk_2 \cos[k_2(B-H)] \sin[k_1 H],$$

$$\mathrm{TM}_p = j\epsilon_2 k_1 \cos[k_2(B-H)] \sin[k_1 H] + j\epsilon_1 k_2 \sin[k_2(B-H)] \cos[k_1 H]. \tag{A5}$$

For the infinite line, the appropriate Green's functions are the same as (A3) except that $\tilde{G}_{ij}$ is replaced by $\tilde{G}_{pij}$.

References

[1] R. A. Pucel, "Design considerations for monolithic microwave circuits," *IEEE Trans. Microwave Theory Tech.*, vol. MTT-29, pp. 513–534, Apr. 1981.

[2] L. Lewin, "A method of avoiding the edge current divergence in perturbation loss calculations," *IEEE Trans. Microwave Theory Tech.*, vol. MTT-32, pp. 717–719, July 1984.

[3] R. A. Pucel, D. J. Masse, and C. P. Harting, "Losses in microstrip," *IEEE Trans. Microwave Theory Tech.*, vol. MTT-16, pp. 342–350, June 1968.

[4] A. Gopinath, "Losses in coplanar waveguides," *IEEE Trans. Microwave Theory Tech.*, vol. MTT-30, pp. 1101–1104, July 1982.

[5] R. Jansen, "Unified user-oriented computation of shielded, covered and open planar microwave and millimeter-wave transmission-line characteristics," *Microwave, Opt. Acoust.*, vol. 3, pp. 14–22, Jan. 1979.

[6] T. Itoh, "Spectral-domain inmittance approach for dispersion characteristics of generalized printed transmission lines," *IEEE Trans. Microwave Theory Tech.*, vol. MTT-28, pp. 733–736, July 1980.

[7] K. C. Gupta, R. Garg, and I. Bahl, *Microstrip Lines and Slotlines*. Dedham, MA: Artech House, 1979.

[8] D. F. Williams and S. E. Schwartz, "A planar subharmonically-pumped 71 Ghz receiver with integral feed antenna," *Int. J. Infrared Millimeter Waves*, vol. 7, no. 2, 1986.

[9] R. W. Jackson and D. M. Pozar, "Surface wave losses at discontinuties in millimeter wave integrated transmission lines," in *IEEE Microwave Symp. Dig.*, June 1985, pp. 563–565.

[10] R. W. Jackson and D. M. Pozar, "Full-wave analysis of microstrip open-end and gap discontinuities," *IEEE Trans. Microwave Theory Tech.*, vol. MTT-33, pp. 1036–1042, Oct. 1985.

[11] R. Jansen, "Hybrid mode analysis of end effects of planar microwave and millimeter transmission lines," *Proc. Inst. Elec. Eng.*, vol. 128, pt.H, pp. 77–86, 1981.

[12] M. Riaziat *et al.*, "Coplanar waveguides used in 2–18 GHz distributed amplifier," in *IEEE Microwave Symp. Dig.*, June 1986, pp. 337–338.

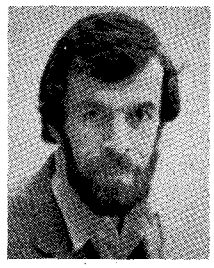

Robert W. Jackson (M'82) was born in Boston, MA, on October 18, 1952. He received the B.S. and Ph.D. degrees in electrical engineering from Northeastern University, Boston, MA, in 1975 and 1981, respectively. His thesis was on nonlinear plasma interactions in the earth's bow shock.

From 1981 to 1982, he was an Assistant Professor at Northeastern University. Since 1982, he has been on the faculty of the Department of Electrical and Computer Engineering at the University of Massachusetts, Amherst, where he is a member of the Microwave and Electronics Laboratory. His research interests include numerical electromagnetics applied to millimeter-wave integrated circuits and active microwave and millimeter-wave circuit design.